Supporting Information

In-Situ Probing Crystal Phase-Dependent Photocatalytic Activities of Au Nanostructures by Surface-Enhanced Raman Spectroscopy

Jingtao Huang,[2] Wenxin Niu,[2,3,4] Cuiling Li,[2] Chaoliang Tan,[2] Pengfei Yin,[1,2] Hongfei Cheng,[2] Zhaoning Hu,[2] Nailiang Yang,[2] Qiyuan He,[5] Gwang-Hyeon Nam,[2] and Hua Zhang*[,1,6]

[1]Department of Chemistry, City University of Hong Kong, Hong Kong, China

[2]Centre for Programmable Materials, School of Materials Science and Engineering, Nanyang Technological University, 50 Nanyang Avenue, Singapore 639798, Singapore

[3]State Key Laboratory of Electroanalytical Chemistry, Changchun Institute of Applied Chemistry, Chinese Academy of Sciences, Changchun 130022, China.

[4]University of Science and Technology of China, Hefei, China.

[5]Department of Materials Science and Engineering, City University of Hong Kong, Hong Kong, China.

[6]Hong Kong Branch of National Precious Metals Material Engineering Research Center (NPMM), City University of Hong Kong, Hong Kong, China.

*Correspondence to: hua.zhang@cityu.edu.hk

EXPERIMENTAL SECTIONS

Materials. Gold(III) chloride trihydrate ($HAuCl_4 \cdot 3H_2O$), silver nitrate, 1,4-benzenedithiol (1,4-BDT), *para*-nitrothiophenol (*p*NTP), hexane, oleylamine, chloroform, 1,2-dichloropropane, L-ascorbic acid and sodium borohydride ($NaBH_4$) were purchased from Sigma-Aldrich. Hexadecyltrimethylammonium bromide (CTAB), sodium oleate (NaOL) were obtained from TCI Chemicals. Hydrochloric acid (HCl, fuming, 37%) was purchased from Merck. All chemicals were used as received without further purification. All aqueous solutions were prepared using Milli-Q water with a resistivity of 18.2 MΩ·cm at room temperature.

Synthesis of 4H Au nanoribbons (NRBs). 4H Au NRBs were synthesized according to our previously reported method with slight modification.[1] In a typical synthesis, 10.62 mL of hexane, 0.66 mL of oleylamine and 0.75 mL of 1,2-dichloropropane were thoroughly mixed in a 20 mL glass vial. Then, 12.24 mg of $HAuCl_4 \cdot 3H_2O$ was added into the vial followed by gentle shaking. The vial was then sealed with PFTE tape and parafilm before being heated for 16 h in an oven pre-set at 58°C. The product was collected by centrifugation (5000 rpm, 3 min), washed with chloroform four times and then re-dispersed in 0.5 mL of chloroform.

Synthesis of *fcc* Au nanowires (NWs). *fcc* Au NWs were synthesized according to a previous method developed for ultrathin Au NWs.[2] In a typical synthesis, 6.4 mg of $HAuCl_4 \cdot 3H_2O$ was dissolved in 3.84 mL of oleylamine in a 20 mL vial under vortex mixing. The resulting amber mixture was then heated for 24 h in an oven pre-set at 58 °C, after which 5.76 mL of chloroform was introduced into the vial. The reaction mixture was heated for another 48 h before being collected by centrifugation (10000 rpm, 20 min). The final product was washed with chloroform three times and re-dispersed in 0.4 mL of chloroform.

Synthesis of *fcc* Au nanorods (NRs). *f*cc Au NRs were prepared according to a seed-mediated approach reported in literature.[3] First, a seed solution for Au NR growth was

prepared by mixing 5 mL of 0.5 mM $HAuCl_4$ with 5 mL of 0.2 M CTAB in a 20 mL glass vial. Then, 1 mL of freshly prepared ice-cold 6 mM $NaBH_4$ was quickly injected into the vial under vigorous stirring. The resultant solution was left undisturbed for 1 h before use. The growth solution of Au NRs was prepared by dissolving 840 mg of CTAB and 148.1 mg of NaOL in 30 mL of deionized water at 30 °C. Then, 2.16 mL of 4 mM $AgNO_3$ was added into the solution and it was left undisturbed for 15 min before 30 mL of 1mM $HAuCl_4$ solution was added. After 90 min of stirring, 0.252 mL of HCl (37%) was added into the solution. 15 min later, 0.15 mL of 0.064 M L-ascorbic acid was introduced under vigorous stirring followed by the addition of 0.096 mL of the seed solution. The resulting mixture was vigorously stirred for 30s and left undisturbed overnight. The product was collected by centrifugation (7000 rpm, 30 min) and washed twice with deionized water before being re-dispersed in 40 mL of deionized water for future use.

Preparation of SERS substrates. The solution of 4H Au NRBs, *fcc* Au NRs and *fcc* Au NWs was drop-cast on silicon wafers. After drying in air, the three Au nanostructures were incubated in 0.1 mM ethanolic solution of *p*NTP overnight. The substrates were rinsed extensively with ethanol so that a monolayer of *p*NTP was formed on the Au surface. After drying in air, the substrates were tested for SERS. The preparation of SERS substrates with 1,4-BDT as probe molecule was similar to that with *p*NTP, except that the substrates were incubated in 10 mM ethanolic solution of 1,4-BDT.

Calculation of enhancement factor (EF). The strongest peak at 1553 cm^{-1} corresponding to the benzene ring mode of 1,4-BDT.[4] was chosen for calculating the EF using the following equation:[5]

$$\mathrm{EF} = \frac{I_{SERS} / N_{SERS}}{I_{Bulk} / N_{Bulk}},$$

where I_{SERS} and I_{Bulk} refer to the SERS intensity of the benzene ring peak and the normal Raman intensity of the peak in powder, respectively; N_{SERS} and N_{Bulk} are the numbers

of 1,4-BDT molecules excited by the laser when they were adsorbed on the Au surface and in powder, respectively. N_{SERS} was calculated by dividing the laser surface area (~ 89.1 μm^2) by the cross-sectional area per molecule (estimated to be 6×10^{-7} μm^2).[6] N_{Bulk} was calculated using the following equation:[7]

$$N_{Bulk} = (V \times D/M) \times N_{A,}$$

where V is the excitation volume (~ 3×10^4 μm^3), D the density of 1,4-BDT powder (1.2 g/cm^3), M the molar mass of 1,4-BDT (142.234 g/mol) and N_A the Avogadro number (6.02×10^{23} /mol). Thus, the average enhancement factors (EFs) were calculated as 1.15×10^8, 1.45×10^7 and 1.28×10^7 for *fcc* Au NRs, 4H Au NRBs and *fcc* Au NWs, respectively.

Electrochemical measurement. Glassy carbon electrodes (GCEs) were successively polished using 0.3 μm and 0.05 μm α-Al_2O_3 powder before they were thoroughly ultrasonicated in deionized water and ethanol for 3 min. Then each of the Au nanostructures in their respective solvents (the mass loading was 3 μg) was dropped onto the GCE surface. After drying in air, the GCEs were subject to ultraviolet (UV) irradiation (254 nm, 10 W) for 4 h to remove remaining surfactants on the Au surface. Then 3 μL of 0.5 wt% ethanolic solution of Nafion was dropped onto the GCE surface and the electrodes were left to dry in air. The electrocatalytic measurement of *p*NTP was conducted by cyclic voltammetry (CV) at a scan rate of 50 mV/s in a mixed solution containing 2 mM *p*NTP and 0.05 M KOH with Ag/AgCl and Pt wire as reference and counter electrodes, respectively.

UV light-catalyzed photocatalytic reaction. 10 μg of the three Au nanostructures were each mixed with 1 mL of a mixed solution containing 2 mM *p*NTP and 0.05 M KOH. The respective solution was transferred into a cuvette, which was subject to UV irradiation (254 nm, 10 W). The reaction was tracked by monitoring the peak at 408 nm with a UV-Vis spectrometer every two minutes. The derived rate constant using first-order reaction rate law indicated the higher photocatalytic activity of 4H Au than that of *fcc* Au in reducing *p*NTP to *p*ATP.[8]

Characterization. Transmission electron microscopy (TEM) images and high-resolution TEM (HRTEM) images were acquired using JEOL JEM-2010 ultrahigh resolution (UHR) and JEM-2100F TEMs operated at 200 kV. Field emission scanning electron microscopy (SEM) images were obtained using a field emission scanning electron microscope (FESEM, JSM-7600F). X-ray diffraction (XRD) patterns were recorded on a Bruker D8 diffractometer at a scan rate of 1°/min with Cu Kα radiation source (λ=1.5406 Å). Ultraviolet-visible (UV-Vis) spectra were collected on a PerkinElmer UV-Vis-NIR Lambda 950 spectrophotometre. SERS measurements were performed on a confocal Raman microscope (WITec Alpha300 SR). The laser wavelength was 785 nm and a 20× objective was used to focus the laser. For excitation of the surface-catalyzed reaction, the laser power was carefully controlled at 17.7±0.2 mW while all the SERS spectra and normal Raman spectra were collected at 1.47 mW laser power, as measured using a laser power meter.

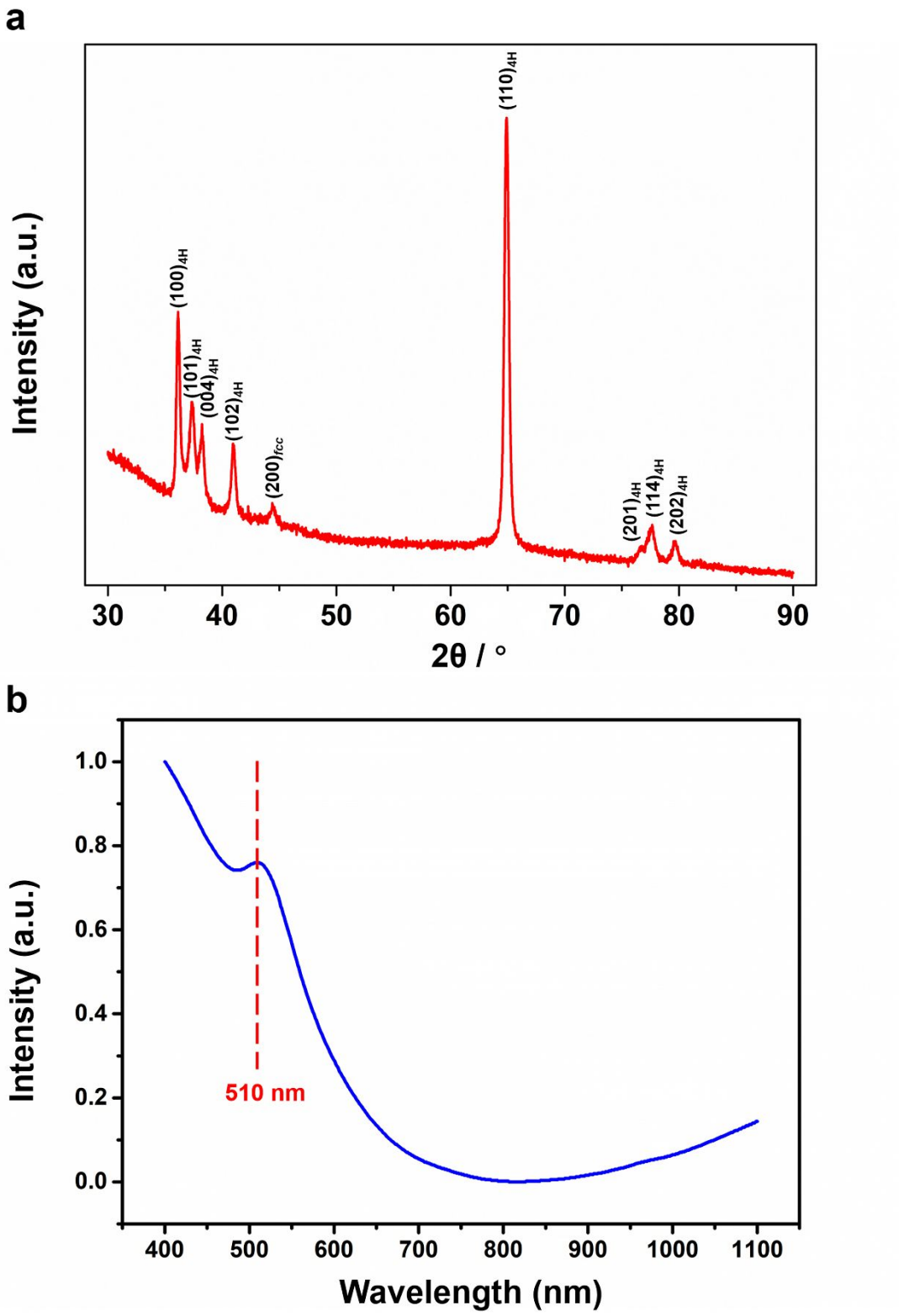
a
Intensity (a.u.)
(100)4H
(101)4H
(004)4H
(102)4H
(200)fcc
(110)4H
(201)4H
(114)4H
(202)4H
30
40
50
60
70
80
90
2θ / °
b
Intensity (a.u.)
1.0
0.8
0.6
0.4
0.2
0.0
510 nm
400
500
600
700
800
900
1000
1100
Wavelength (nm)

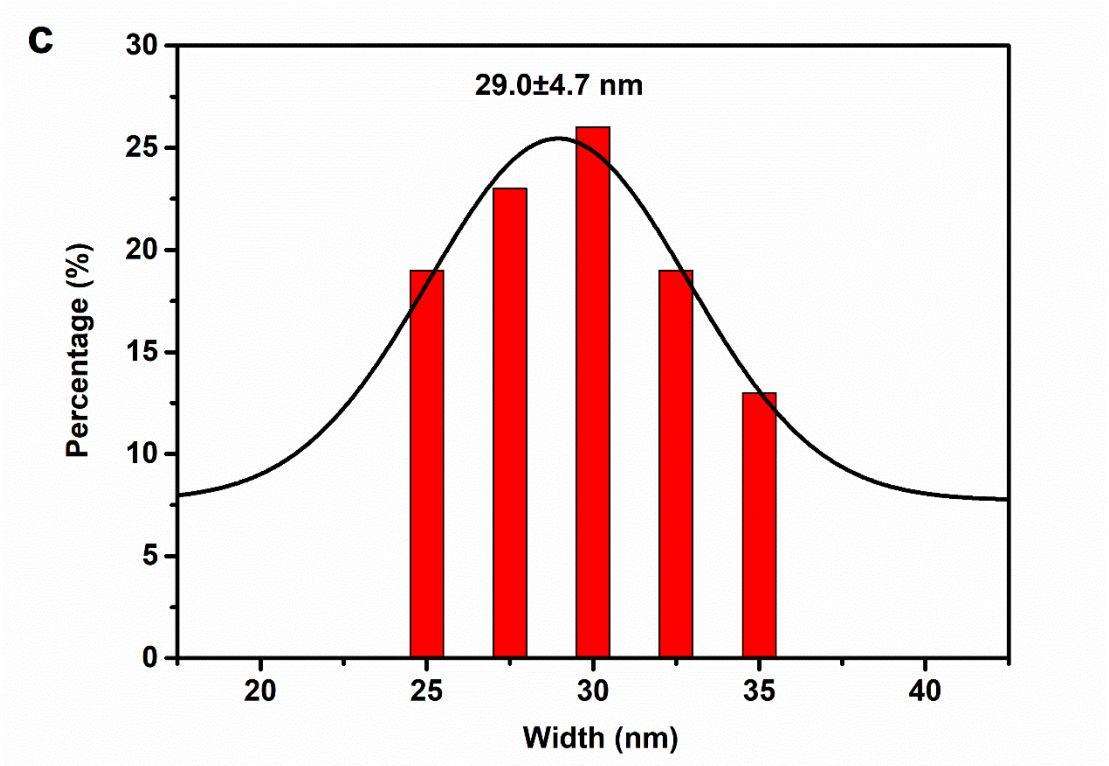

Figure S1. (a) The XRD pattern of the 4H Au NRBs. Note that the peak at 44° corresponds to the small amount of by product, *i.e.* the *fcc* Au nanoparticles. (b) Normalized extinction spectrum of the Au NRBs with a transverse SPR peak at 510 nm. (c) Histogram of the width of 4H Au NRBs

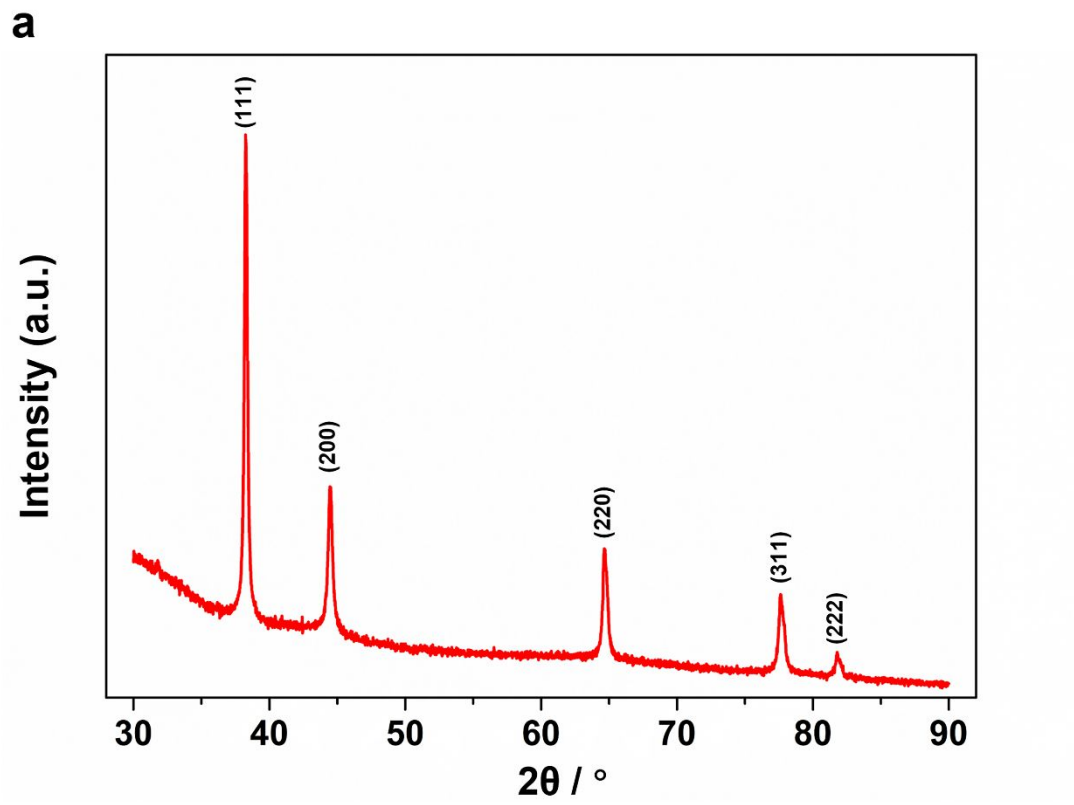
a
Intensity (a.u.)
(111)
(200)
(220)
(311)
(222)
30
40
50
60
70
80
90
2θ / °

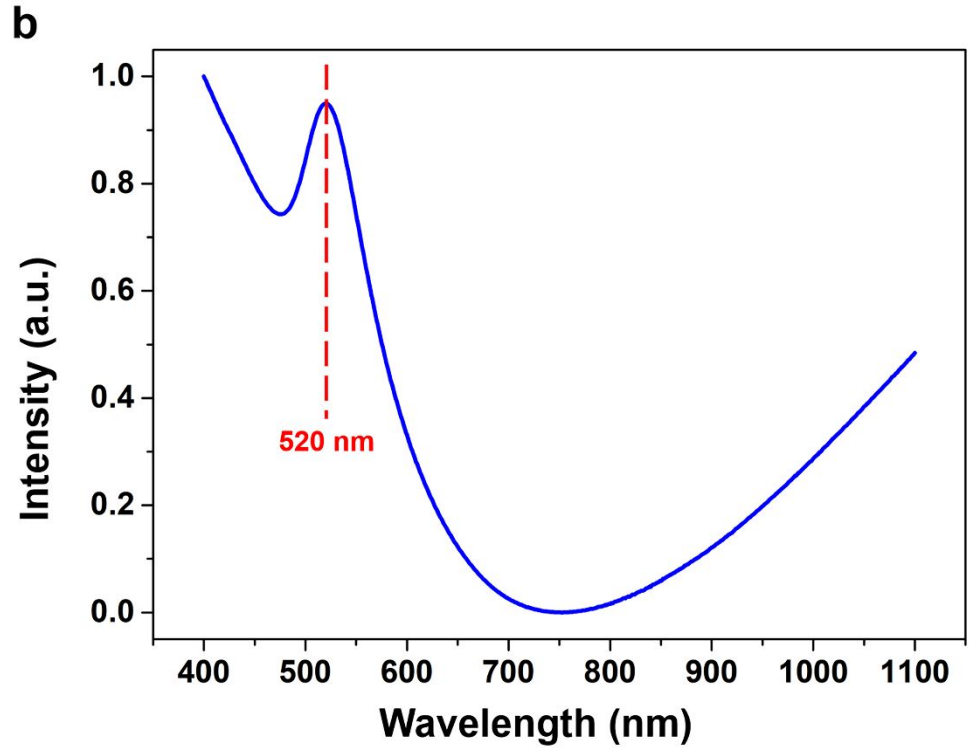
b
Intensity (a.u.)
1.0
0.8
0.6
0.4
0.2
0.0
520 nm
400
500
600
700
800
900
1000
1100
Wavelength (nm)

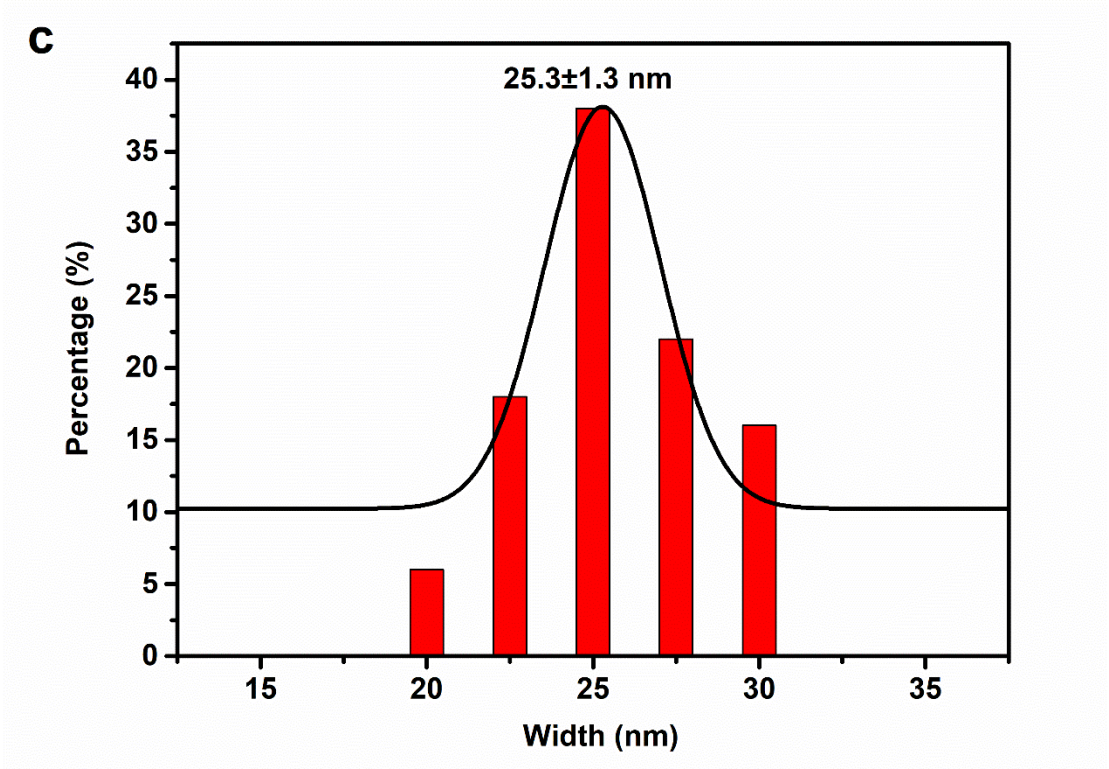

Figure S2. (a) The XRD pattern of the *fcc* Au NWs. (b) Normalized extinction spectrum of the *fcc* Au NWs with a transverse SPR peak at 520 nm. (c) Histogram of the width of *fcc* Au NWs.

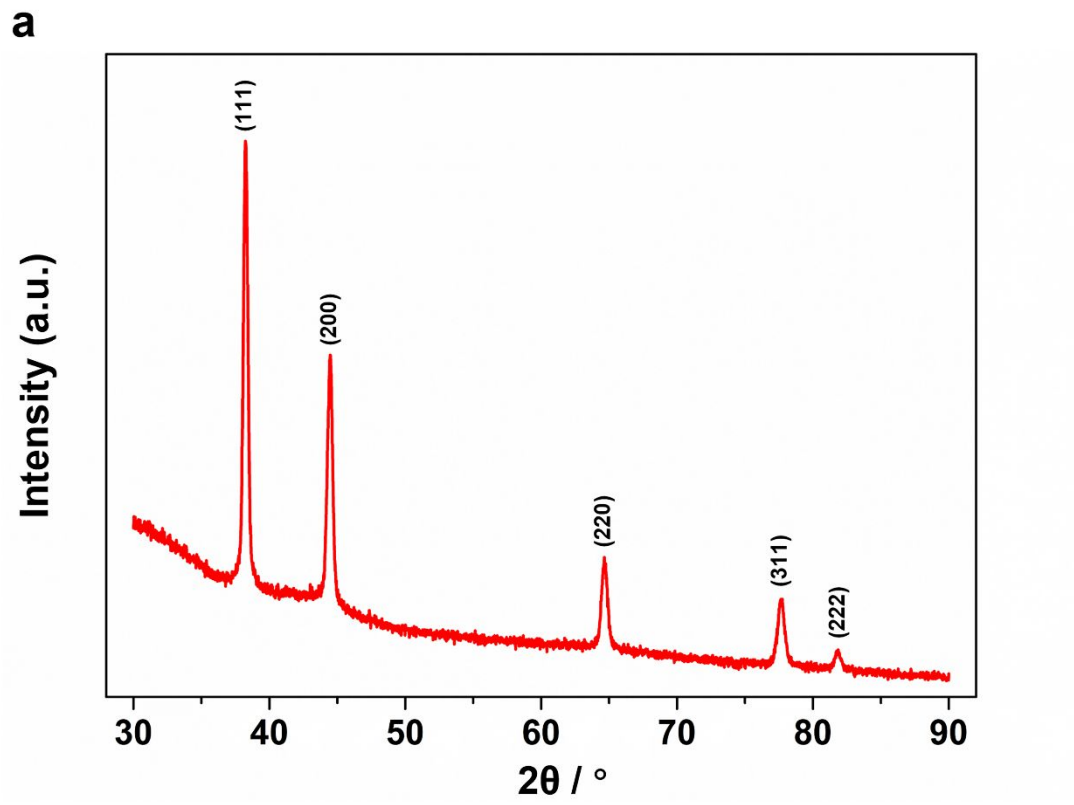
a
(111)
(200)
(220)
(311)
(222)
Intensity (a.u.)
30
40
50
60
70
80
90
2θ / °

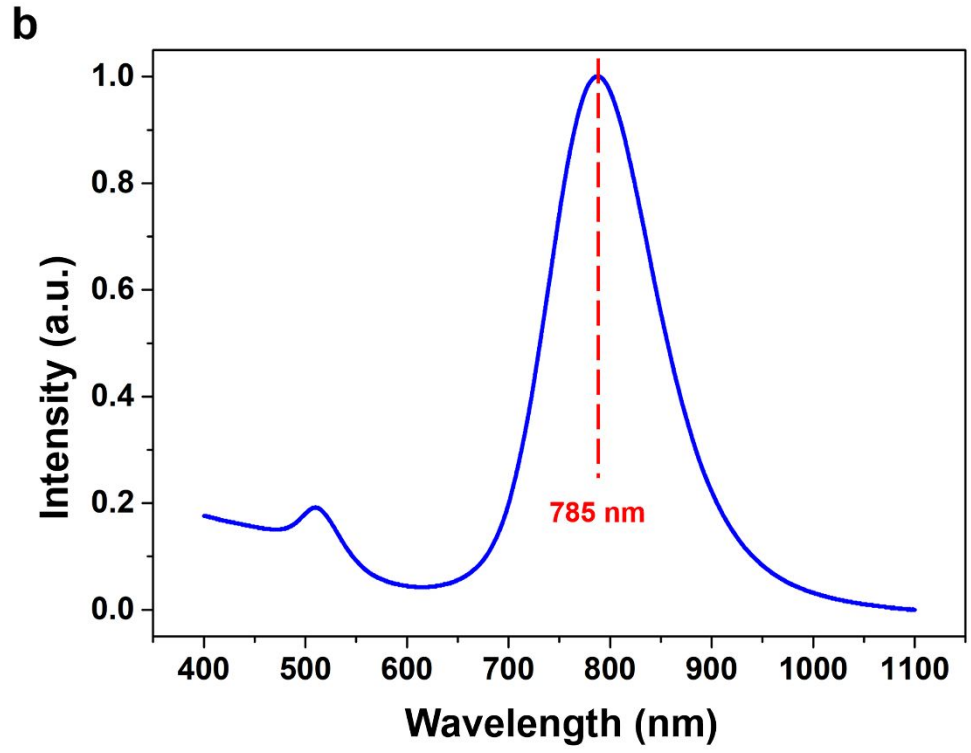
b
1.0
0.8
0.6
0.4
0.2
0.0
Intensity (a.u.)
785 nm
400
500
600
700
800
900
1000
1100
Wavelength (nm)

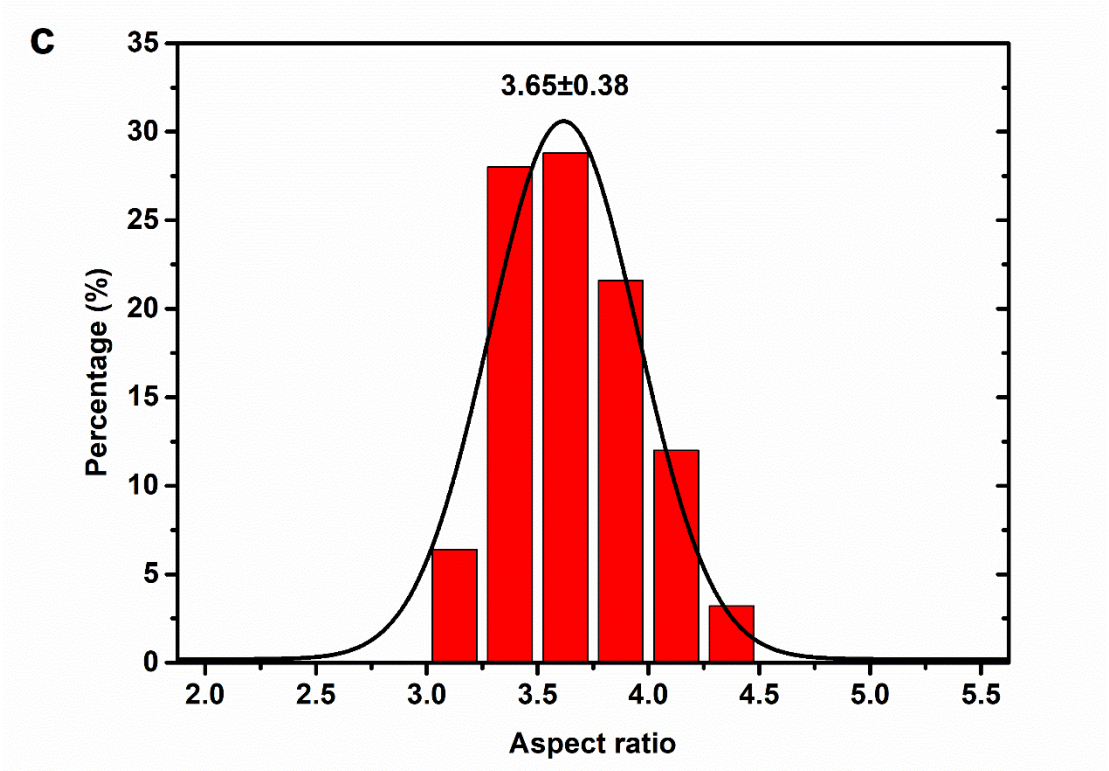

Figure S3. (a) The XRD pattern of the *fcc* Au NR**.** (b) Normalized extinction spectrum of the *fcc* Au NRs with a longitudinal SPR peak at 785 nm. (c) Histogram of the aspect ratio of *fcc* Au NRs.

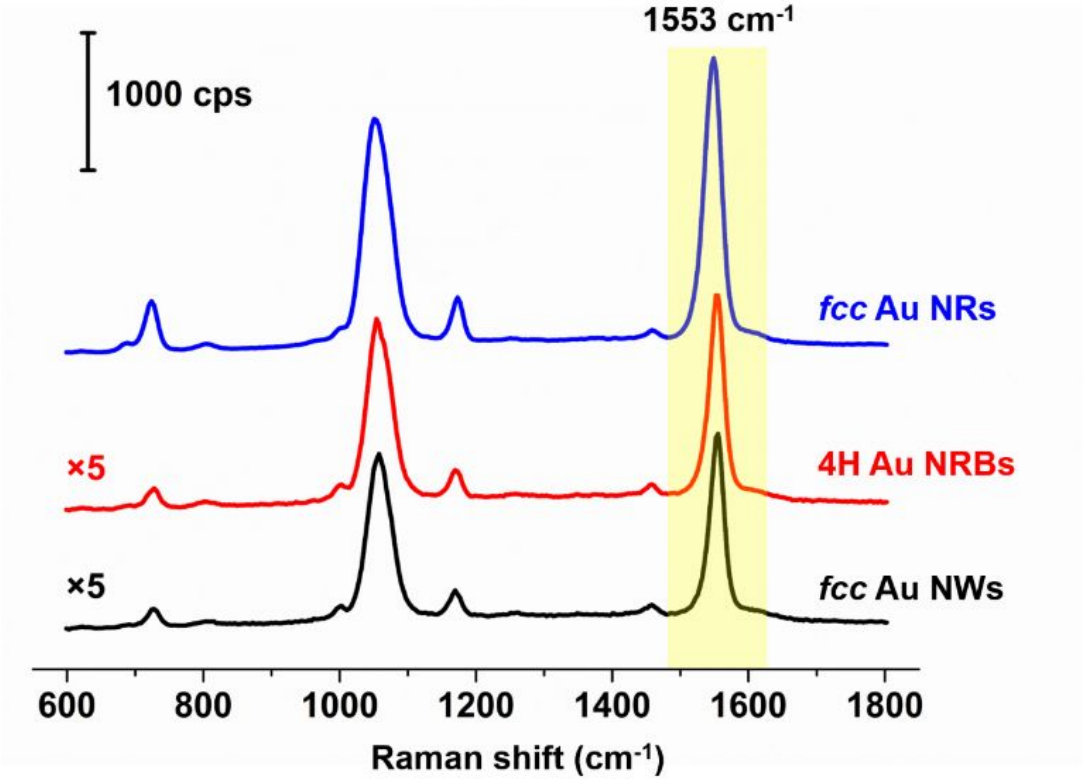

Figure S4. SERS spectra collected from 1,4-BDT adsorbed on the three types of Au nanostructures at the excitation of 785 nm laser (1.47 mW). Each spectrum is the average of spectra taken on 12 randomly selected positions. The enhancement factors were calculated based on the benzene ring mode at 1553 cm^{-1}.

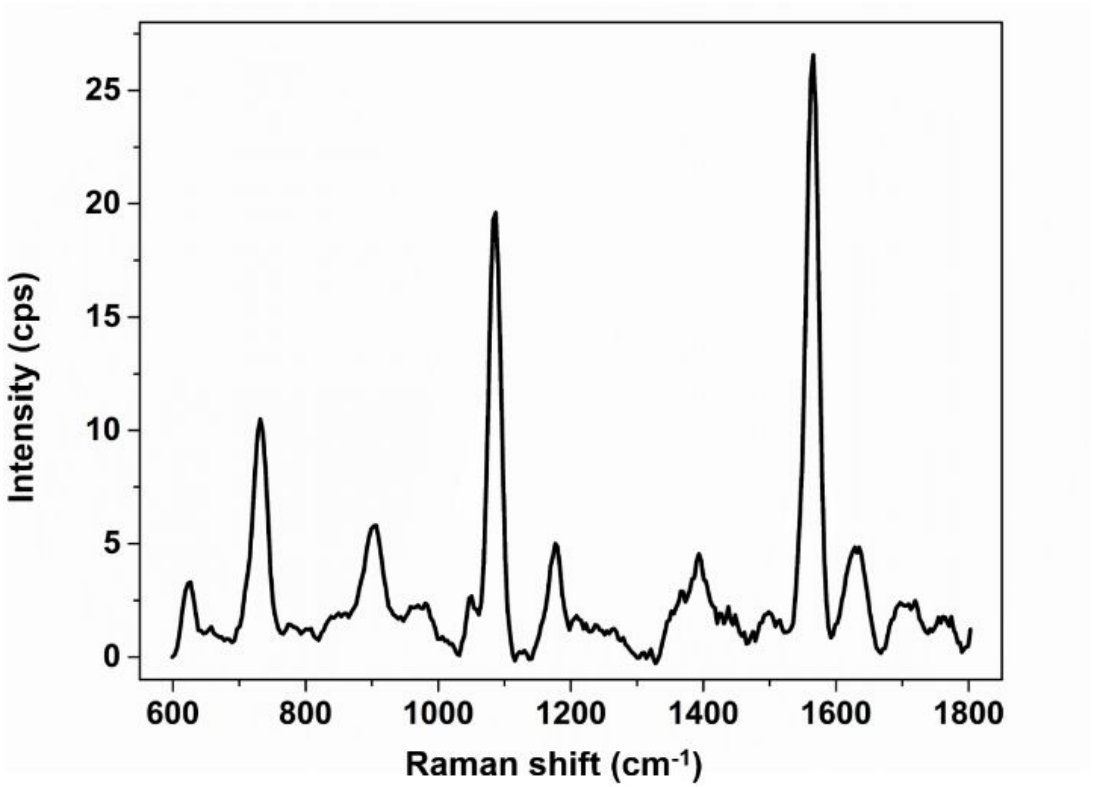

Figure S5. Normal Raman spectrum of 1,4-BDT powder on a glass slide collected using 785 nm laser at low power, *i.e.* 1.47 mW.

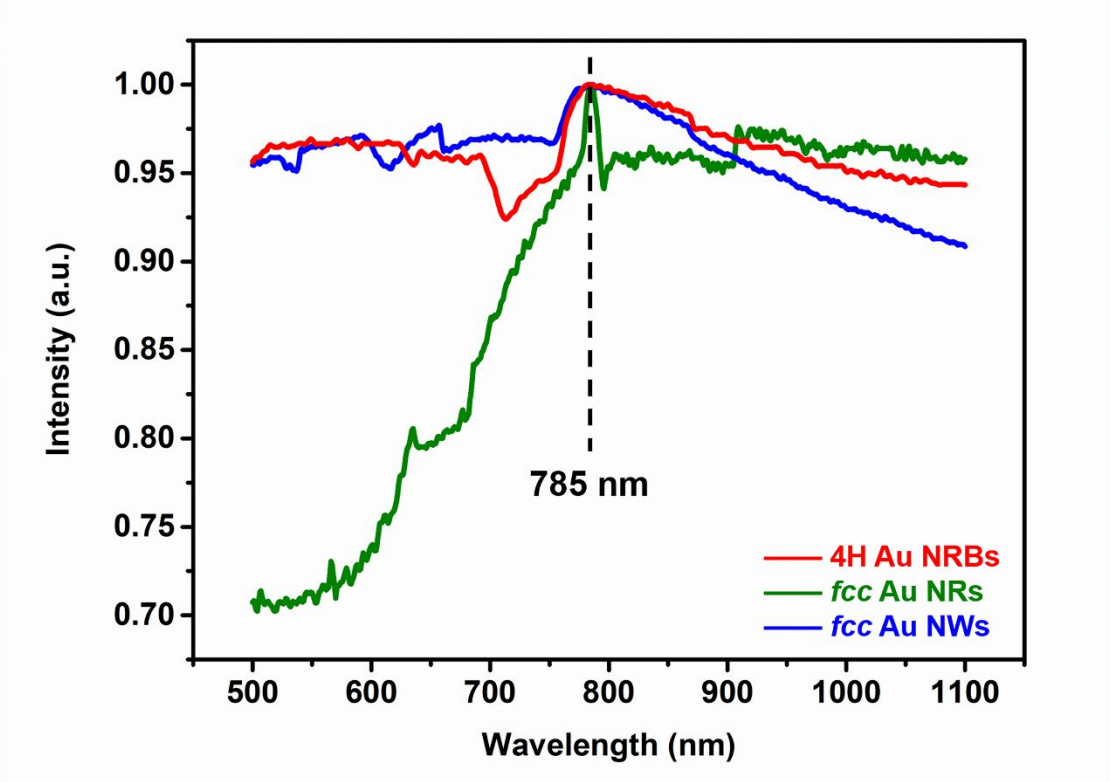

Figure S6. Normalized extinction spectra measured on the films of 4H Au NRBs, *fcc* Au NRs and *fcc* Au NWs. The films were used for the *in-situ* SERS studies in Figure 2. The dashed line shows that 785 nm laser was in resonance with the plasmon peaks of the three Au nanostructures.

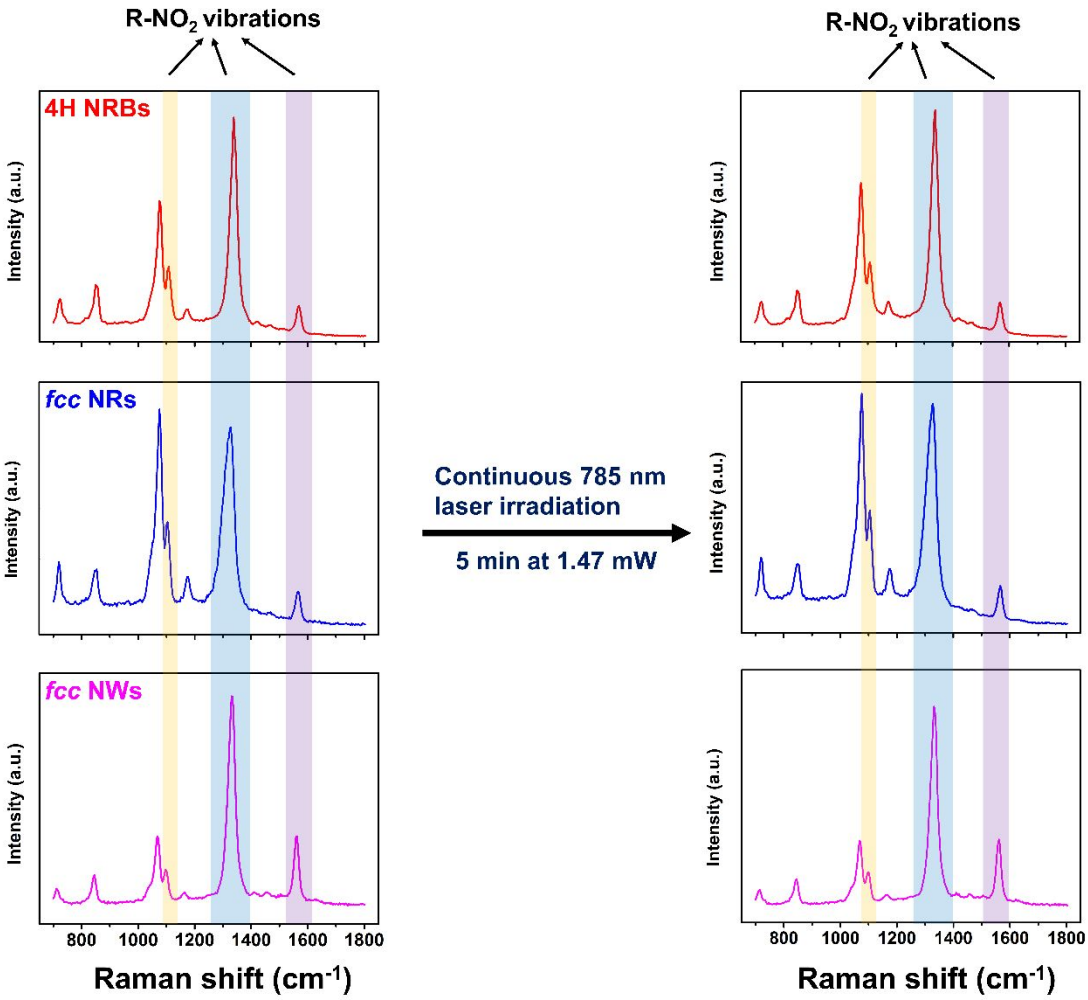

Figure S7. SERS spectra of *p*NTP adsorbed on the three types of Au nanostructures collected before (left panel) and after (right panel) 5 min of 785 nm laser irradiation at low power (1.47 mW). No spectral changes were observed after the low-power laser irradiation, indicating that this low laser power (1.47 mW) is suitable for *in-situ* probing the reaction.

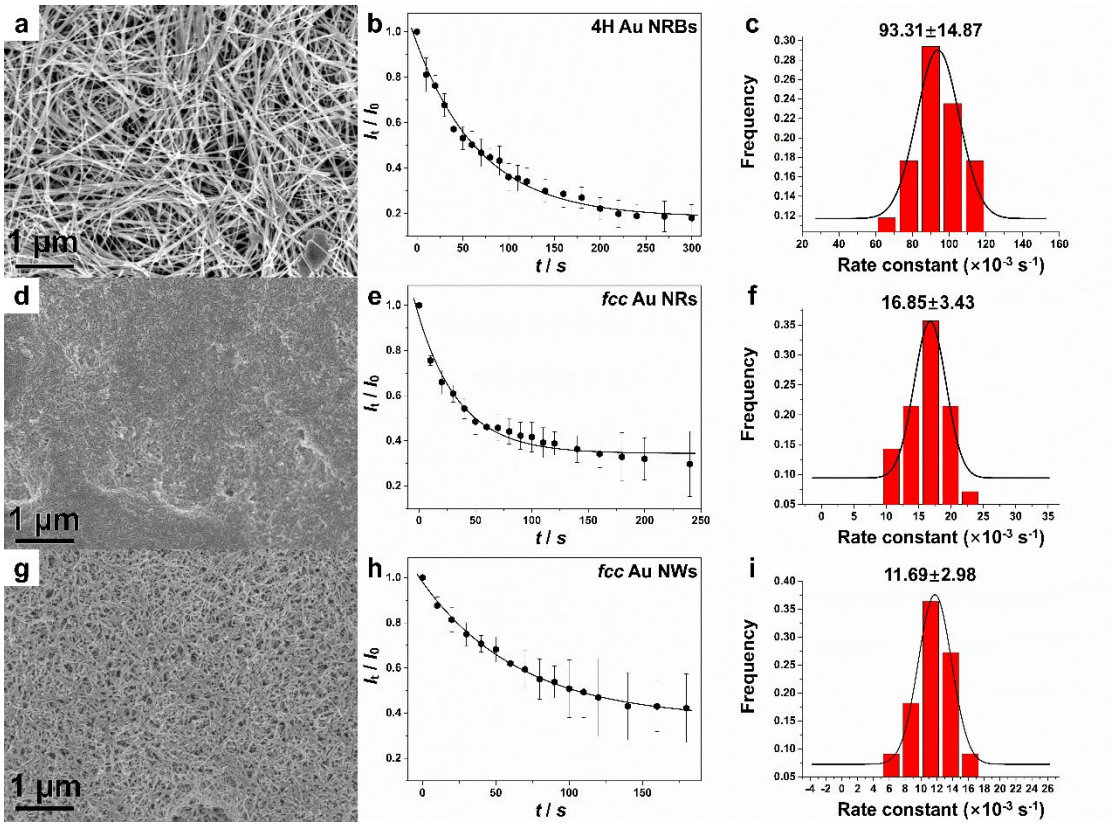

Figure S8. SEM images of (a) 4H Au NRBs, (d) *fcc* Au NRs, and (g) *fcc* Au NWs used in the *in-situ* SERS experiments. Relative SERS intensity change in the O-N-O stretching vibrational band at 1338 cm^{-1} as a function of time for (b) 4H Au NRBs, (e) *fcc* Au NRs, and (h) *fcc* Au NWs. Histogram of the rate constant distribution for the photocatalytic reaction on (c) 4H Au NRBs, (f) *fcc* Au NRs, and (i) *fcc* Au NWs.

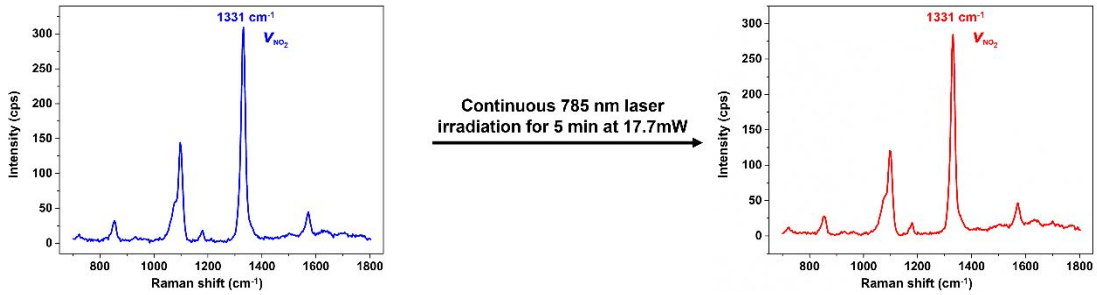

Figure S9. Normal Raman spectra of the *p*NTP powder on a glass slide before (left panel) and after (right panel) 785 nm laser irradiation for 5 min at high power (17.7 mW). Both the spectra were collected using 785 nm laser at 1.47 mW. In the absence of plasmonic Au, no hot electron-induced conversion of *p*NTP to DMAB was observed.

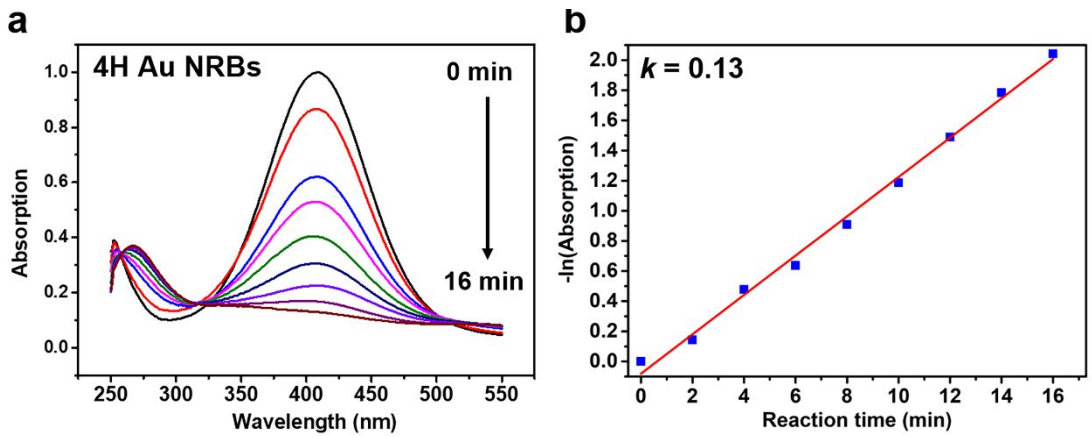

Figure S10. UV-catalyzed reduction of *p*NTP in the presence of 4H Au NRBs. (a) UV-Vis monitoring of the reduction at an interval of 2 min. (b) Linear fit of -ln(absorption) versus reaction time demonstrates the reaction follows first order kinetics with a rate constant of 0.13 min^{-1}.

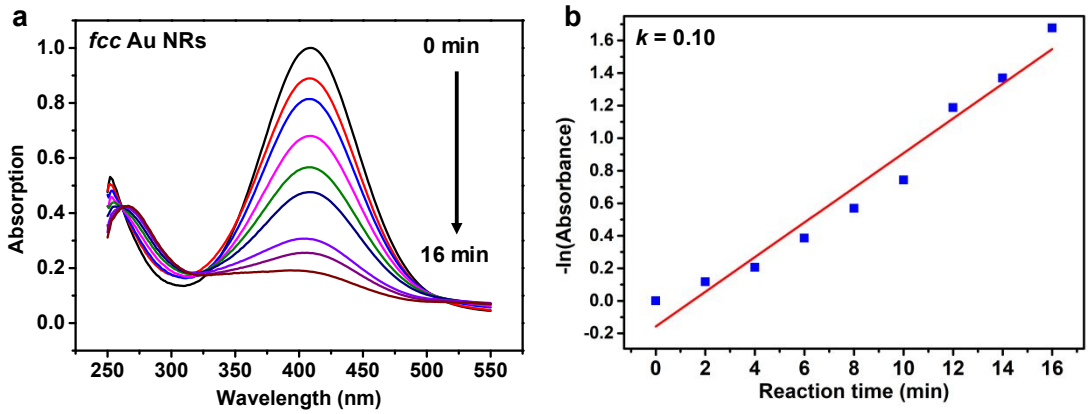

Figure S11. UV-catalyzed reduction of *p*NTP in the presence of *fcc* Au NRs. (a) UV-Vis monitoring of the reduction at an interval of 2 min. (b) Linear fit of -ln(absorption) versus reaction time demonstrates the reaction follows first order kinetics with a rate constant of 0.10 min^{-1}.

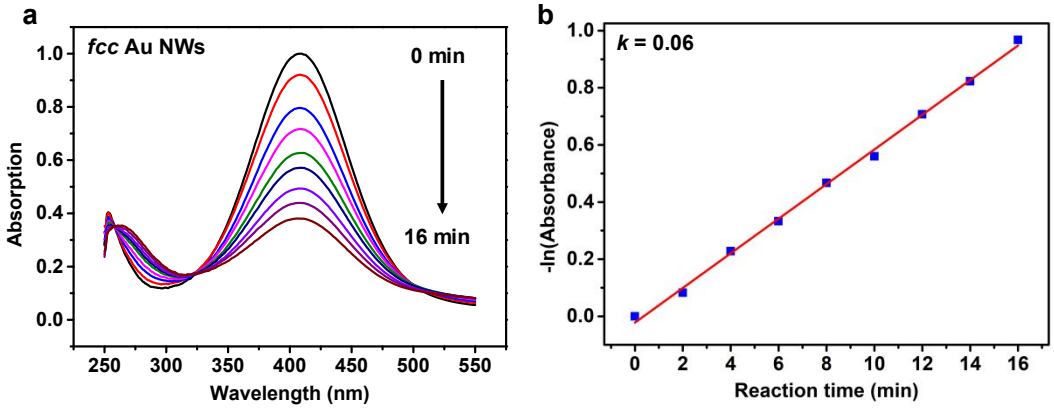

Figure S12. UV-catalyzed reduction of *p*NTP in the presence of *fcc* Au NWs. (a) UV-Vis monitoring of the reduction at an interval of 2 min. (b) Linear fit of -ln(absorption) versus reaction time demonstrates the reaction follows first order kinetics with a rate constant of 0.06 min^{-1}.

References

(1) Niu, W. X.; Liu, J. W.; Huang, J. T.; Chen, B.; He, Q. Y.; Wang, A. L.; Lu, Q. P.; Chen, Y.; Yun, Q. B.; Wang, J.; Li, C. L.; Huang, Y.; Lai, Z. C.; Fan, Z. X.; Wu, X. J.; Zhang, H. Unusual 4H-Phase Twinned Noble Metal Nanokites. *Nat. Commun.* **2019**, *10*, 2881.

(2) Pazos-Perez, N.; Baranov, D.; Irsen, S.; Hilgendorff, M.; Liz-Marzan, L. M.; Giersig, M. Synthesis of Flexible, Ultrathin Gold Nanowires in Organic Media. *Langmuir* **2008**, *24*, 9855-9860.

(3) Ye, X. C.; Zheng, C.; Chen, J.; Gao, Y. Z.; Murray, C. B. Using Binary Surfactant Mixtures To Simultaneously Improve the Dimensional Tunability and Monodispersity in the Seeded Growth of Gold Nanorods. *Nano Lett.* **2013**, *13*, 765-771.

(4) Yin, Z.; Wang, Y.; Song, C. Q.; Zheng, L. H.; Ma, N.; Liu, X.; Li, S. W.; Lin, L. L.; Li, M. Z.; Xu, Y.; Li, W. Z.; Hu, G.; Fang, Z. Y.; Ma, D. Hybrid Au-Ag Nanostructures for Enhanced Plasmon-Driven Catalytic Selective Hydrogenation Through Visible Light Irradiation and Surface-Enhanced Raman Scattering. *J. Am. Chem. Soc.* **2018**, *140*, 864-867.

(5) Cardinal, M. F.; Ende, E. V.; Hackler, R. A.; McAnally, M. O.; Stair, P. C.; Schatz, G. C.; Van Duyne, R. P. Expanding Applications of SERS Through Versatile Nanomaterials Engineering. *Chem. Soc. Rev.* **2017**, *46*, 3886-3903.

(6) Soriaga, M. P.; Hubbard, A. T. Determination of the Orientation of Adsorbed Molecules at Solid-Liquid Interfaces by Thin-Layer Electrochemistry: Aromatic-Compounds at Platinum-Electrodes. *J. Am. Chem. Soc.* **1982**, *104*, 2735-2742.

(7) Villarreal, E.; Li, G. F. G.; Zhang, Q. F.; Fu, X. Q.; Wang, H. Nanoscale Surface Curvature Effects on Ligand-Nanoparticle Interactions: A Plasmon-Enhanced Spectroscopic Study of Thiolated Ligand Adsorption, Desorption, and Exchange on Gold Nanoparticles. *Nano Lett.* **2017**, *17*, 4443-4452.

(8) Joseph, V.; Engelbrekt, C.; Zhang, J. D.; Gernert, U.; Ulstrup, J.; Kneipp, J. Characterizing the Kinetics of Nanoparticle-Catalyzed Reactions by Surface-Enhanced Raman Scattering. *Angew. Chem. Int. Ed.* **2012**, *51*, 7592-7596.